Photoluminescence study of the dynamical properties of GaAs sawtooth superlattices

M. B. Johnston[a] and M. Gal[b]
School of Physics, The University of New South Wales, Sydney NSW 2052, Australia

G. Li and C. Jagadish
Department of Electronic Materials Engineering, The Research School of Physical Sciences and Engineering, The Institute of Advanced Studies, The Australian National University, Canberra ACT 0200, Australia

(Received 6 March 1997; accepted for publication 16 August 1997)

The dynamic properties of a sawtooth superlattice (δ-doped *nipi*) were examined by photoluminescence (PL) spectroscopic techniques. The structure was grown on a semi-insulating GaAs substrate by metalorganic vapor phase epitaxy, using C and Si δ-doping. The excitation intensity dependence of the sample's PL was measured over six decades which produced a shift of 200 meV in the peak of the PL photon energy. The dynamic properties of the sawtooth superlattice were probed using time resolved PL and carrier lifetime measurements. Time resolved PL was measured over 6 orders of magnitude in delay time. The luminescence wavelength from the sawtooth superlattice sample was found to shift to low energies over time after pulsed excitation, indicating the temporal evolution of the band edges. A new and sensitive technique for measuring radiative recombination lifetimes at low excitation intensities was developed. Therefore δ-doped sawtooth superlattices are shown to have a tunable band gap as well as an intensity tunable carrier lifetime. © *1997 American Institute of Physics.* [S0021-8979(97)07422-7]

I. INTRODUCTION

Doping *nipi* superlattice structures were first hypothesised by Esaki and Tsu[1] in 1970. The δ-doped *nipi* superlattice (sawtooth superlattice) was theoretically analyzed in 1972 by Döhler,[2] however some of the first experimental verification of this work had to wait until a sawtooth superlattice could be grown reliably.[3] These early δ-doped *nipi* structures were grown by molecular beam epitaxy. More recently a technique has been developed to grow these structures using metalorganic vapor phase epitaxy (MOVPE).[4]

Considerably more experimental work has been conducted on homogeneously doped *nipi* superlattices[5] since the growth of such structures was realized in the early 1980's. Sawtooth superlattices and homogeneously doped *nipi* structures share the following features: tunable band gaps at energies below that of the bulk; long carrier recombination lifetimes, and strong nonlinearity. Sawtooth superlattice structures however have shown improved optical properties over homogeneously doped *nipi* superlattices.[6]

A δ-doped *nipi* superlattice is a semiconductor crystal structure in which the spatial band structure is modulated by periodic internal electric fields. The variation of electric field in the growth direction is a result of alternating sheets of *n* and *p* type ionized dopants separated by undoped semiconductor (Fig. 1). The sheets are produced by a δ-doping process during epitaxial growth of the sample. Dopants are confined to within a layer with dimension of the order of the crystal lattice constant. In contrast, the electric field modulation of a homogeneously doped structure is established via a continuous (rather then δ-function like) variation of *n*- and *p*-dopant concentration over each period of the structure.

Homogeneously doped structures suffer from potential fluctuations across the sample[6] since local electric field variations are associated with any statistical distribution of dopants. Sawtooth superlattices are immune from this problem since the doping layers make up a small proportion of the structure's volume. The regions between the doping planes contain effectively no impurities and are subject to smooth linear electric fields. Quantum well heterostructures can be incorporated in these undoped regions, confining carriers away from the impurities. Such structures are termed hetero-*nipi*s.[7]

Sawtooth superlattices show promise in device applications such as tunable light emitting diodes and lasers.[8] Infrared subband detectors and modulators incorporating δ-doped *nipi* structures have also been theoretically investigated.[9] At present much interest is also focused on nonlinearity in hetero-*nipi*s[10] with possible application to all optical computing.[11]

The unique properties of sawtooth superlattices result from the confinement of electrons and holes within the triangular potential well produced by the internal electric field. Holes and electrons are spatially separated in the growth direction, which leads to long radiative recombination lifetimes. A long lifetime of carriers amplifies band-filling effects and the screening of the periodic electric field.

The *effective bandgap* of an *nipi* is the energy gap between the ground state electron and ground hole states in its triangular potential wells. The effective band-gap energy is usually below that of the bulk semiconductor, but approaches the band gap of the bulk when the field associated with the δ-doped layers is screened.

Understanding the fundamental dynamics of sawtooth superlattices is clearly important in device applications. An

[a]Electronic mail: mbj@newt.phys.unsw.edu.au
[b]Electronic mail: m.gal@unsw.edu.au

 0021-8979/97/82(11)/5748/5/$10.00

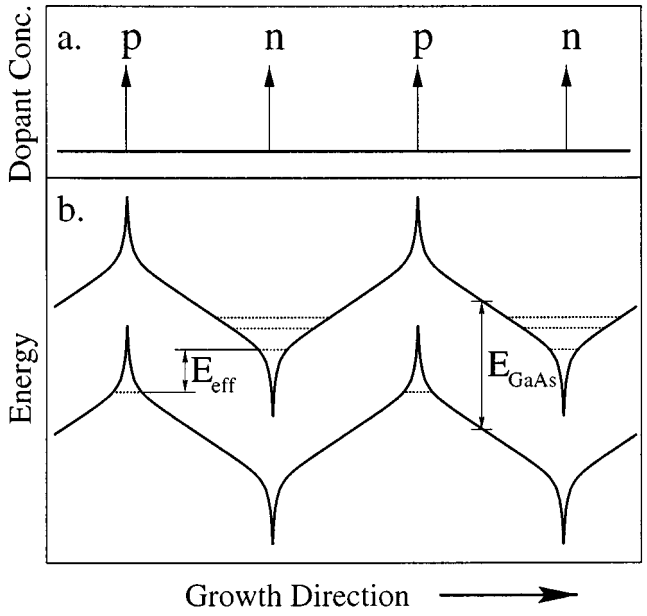

FIG. 1. Schematic diagram of (a) the doping profile and (b) the band structure of an (unexcited) δ-doped sawtooth superlattice. In (a) delta functions are used to represent the high concentration of *n*- or *p*-type dopants. The spatial scale in (b) is exaggerated around the doped layers to emphasize the deep potential wells formed by δ-doping. Note how the effective band gap of the structure, E_{eff}, is narrower than the band gap (E_{GaAs}) of bulk GaAs.

early study of the dynamics of conventional *nipi* superlattices[12] found large shifts in band gap energy during relaxation processes. Lifetime studies have also been carried out on hetero-*nipi* structures using differential transmission techniques[10,13] with significant discrepancies between theory and experiment. A systematic investigation and understanding of simple sawtooth superlattices is a necessary step before more complex structures can be understood.

II. SAMPLE GROWTH

The growth of δ-doped GaAs superlattice structures by metalorganic vapor phase epitaxy (MOVPE) has been described previously.[4] Briefly, silane and trimethylaluminium were used as *n* (Si) and *p* (C) type doping precursors, respectively. The δ-doped sawtooth superlattice described herein had an intrinsic layer thickness of 30 nm between *n*- and *p* type δ-doped layers. Ten of these 60 nm periods were grown and capped with 30 nm of intrinsic GaAs. The growth temperature was 630 °C.

The sheet density of Si and C δ-doped layers is $\approx 2 \times 10^{12}\ \text{cm}^{-2}$. The corresponding full carrier profile width at half maximum is about 5.5 nm for Si and 7.5 nm for C δ-doped layers. Referring to the depth resolution of capacitance–voltage profiling in δ-doped semiconductors,[14] the dopants in those δ-doped layers are apparently confined to a couple of monolayers.

III. EXPERIMENT

Three different photoluminescence (PL) techniques were used to probe the dynamics of the sawtooth superlattice's band edges, since PL is ideal for measuring the position of the effective band gap in an *nipi* structure.

(a) cw photoluminescence data were acquired using a 0.27 m spectrometer and a cooled (silicon) charged coupled device (CCD) array. The sample was excited using an unchopped CW argon laser ($\lambda = 488$ nm). The intensity of the illumination was varied using neutral density filters. This technique provides information about the effective bandgap of *nipi*s as a function of excitation intensity.

(b) Time resolved photoluminescence (TRPL) spectra were obtained at a range of times after a 500 ps 10 μJ pulse from a nitrogen-dye laser ($\lambda \approx 500$ nm) using a 0.75 m spectrometer. The spectrally resolved signal was detected using a photomultiplier tube with an S1 photocathode and 50 Ω termination. A silicon photodiode was used for measuring slow, low intensity decays. A boxcar averager interfaced to a personal computer was used to record the TRPL spectra. The boxcar was triggered via a fast silicon photodiode using a component of the pulse reflected from the quartz window of the cryostat. The effective band gap as a function of time after pulsed excitation reveals the relaxation of the excited *nipi* band edge.

(c) Radiative recombinatation lifetimes were measured using modulated PL. In this new technique the beam from a continuous wave argon laser ($\lambda = 488$ nm) was sinusoidally modulated using an acousto-optic modulator (AOM). The AOM was driven by the sine wave from the internal signal generator of a lock-in amplier. The modulation depth of the laser was controlled by providing a dc offset to the sine wave signal before it reached the AOM. The PL signal was detected using an S1 PMT (5.6 kΩ termination) after it had been dispersed using a spectrometer. The frequency of modulation and detection was scanned logarithmically from 100 Hz to 100 kHz in 200 steps. These data points were used to deduce the *nipi*'s electron-hole recombination lifetime at the emission energy set by the spectrometer.

In all the PL techniques the temperature of the sample was maintained at 10 K. In each case the laser was focused onto a 2 mm diameter spot on the sample. The PL was collected from the center of this spot, where excitation was approximately uniform.

IV. EFFECT OF LASER INTENSITY

Observing a blue shift in PL spectra with increasing excitation intensity has long been a method of identifying *nipi* behavior.[5,8,12] The intensity dependence of continuous-wave PL spectra was measured over 6 orders of magnitude. The normalized PL spectra over this intensity range are shown in Fig. 2.

At high excitation intensity the peak of the PL spectrum, which corresponds to the *nipi*'s effective band gap, approaches the GaAs band-gap energy (1.52 eV at 10 K). In this case the internal electric field has been fully shielded by the photoinduced carriers, therefore sawtooth potential wells

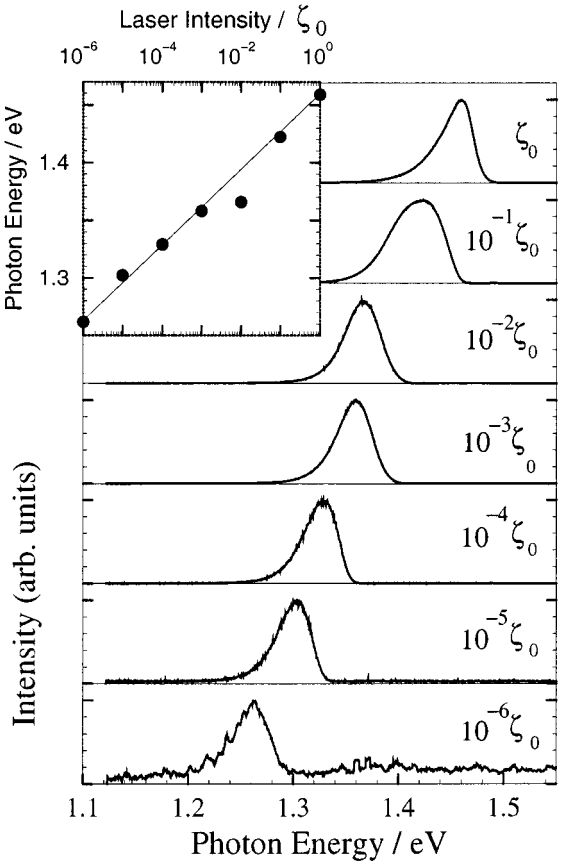

FIG. 2. Excitation intensity dependence of PL spectra from a δ-doped sawtooth superlattice, ζ_0 was the intensity of unattenuated laser light on the sample ($\zeta_0 \approx 7$ mW/mm^2). Inset: Shift of PL maxima as a function of excitation intensity (the line is an aid to the eye).

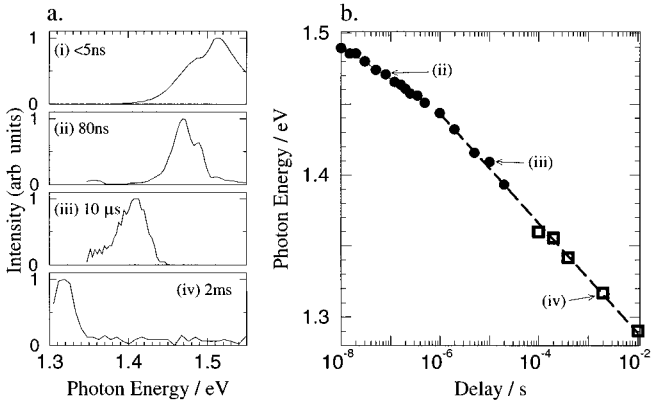

FIG. 3. Relaxation of *nipi* after pulsed excitation. (a) Shows some time resolved PL results for a δ-doped sawtooth superlattice. (b) Summarizes TRPL data, showing peak PL emission energy of each time resolved PL spectrum as a function of delay time. Points marked with (●) were measured using an S1 photomultiplier tube, while those marked with (□) were measured with a silicon photodiode. Two logarithmic regressions are shown (solid and dashed lines).

disappear. At lower excitation intensity the PL spectra show maxima at lower energies, indicating a decrease in the effective band-gap energy of the *nipi* structure.

An overall shift in PL maxima from 1.26 eV ($\lambda = 984$ nm) to 1.46 eV ($\lambda = 849$ nm) was observed. This 200 meV shift is comparable with shifts measured on a similar structure grown by molecular beam epitaxy.[3] Note that a similar shift was also observed from a homogeneously doped *nipi* superlattice at room temperature[15] (albeit with much broader PL spectra). Clearly the MOVPE grown δ-doped sawtooth superlattice shows well established *nipi* behavior.

V. RELAXATION OF BAND EDGES

The time resolved photoluminescence (TRPL) experiment using a pulsed laser was conducted to observe the temporal evolution of band edge relaxation in a sawtooth superlattice. The technique allowed a series of PL spectra to be recorded during the course of *nipi* band edge relaxation, after pulsed excitation. In this work, a short (500 ps) laser pulse was used to produce free carriers, and then the relaxation of the system, *without* the laser beam's electric field, was measured via PL spectroscopy. The delay time ranged over 6 orders of magnitude (10 ns–10 ms). Figure 3(a) shows a number of the TRPL spectra which were recorded at selected delay times after the pulsed excitation.

Figure 3(a)(i) is the PL spectrum of a δ-doped sawtooth superlattice immediately after excitation (i.e., during the first 5 ns after the pulse). Note the tail to the high energy side of the broad GaAs band-gap energy peak. The tail is characteristic of an electron-hole plasma in an intensely excited semiconductor. The PL peak is close to the GaAs band gap since the carriers from the plasma completely shield the characteristic *nipi* electric field (associated with ionized dopants). In this case, the effective band gap and carrier recombination lifetimes are similar to those of the bulk.

Figures 3(a)(ii)–(iv) are examples of PL spectra recorded at later times after excitation. The PL emission shifts from high to low energy as a function of delay time, with full width half-maxima less than 40 meV. A summary of many of these spectra is provided in Fig. 3(b).

After pulsed excitation the *nipi*'s effective band gap reduces with increasing delay. This is a result of a strengthening of the *nipi* internal electric field via electron-hole pair recombination. This process has been regarded as relaxation of excited *nipi* structures in this work.

It has been observed that the relaxation of the effective band gap of a *nipi* occurs with two logarithmic decay times [see Fig. 3(b)]. In the first microsecond after excitation a long (logarithmic) relaxation constant is observed, while in the period following this the structure relaxes with a greater logarithmic decay constant.

VI. RECOMBINATION LIFETIME

An alternative way of observing the dynamics of a sawtooth superlattices is to measure the radiative recombination or PL lifetime of its carriers. Most conventional carrier lifetime measurements use short, high intensity laser pulses to excite a sample. These types of measurements are clearly not suitable for measuring *nipi* structures at low excitation intensities.

A technique has been developed to measure the radiative recombination, or PL lifetime of a sawtooth superlattice over

a large range of excitation intensities, with two independent variables: the exciting beam's intensity, and the sample's emission wavelength. It is also very sensitive and therefore allowed measurements to be taken at photon energies where the PL intensity was low.

In this technique the intensity of the laser light, $\zeta_e(t)$ was sinusoidally modulated, to a modulation depth, m, by an acousto-optic modulator at frequencies, $\hat{\omega}/2\pi$, between 100 Hz and 100 kHz. That is,

$$\zeta_e(t)=\zeta_0\left(1-\frac{m}{2}(1-\sin\hat{\omega}t)\right) \tag{1}$$

where ζ_0 is the maximum laser intensity. For low intensities it was assumed that the number of electron-hole pairs created in the sample is proportional to the exciting intensity, $\zeta_e(t)$, of the laser. Furthermore if the carriers recombine radiatively with an exponential decay time, τ, then the PL from the sample may be expressed as

$$\zeta_r(t)=\eta N\int_{-\infty}^{t}\zeta_e(t')\exp\frac{-(t-t')}{\tau}dt' \tag{2}$$

since the PL signal at time t is the sum of the decaying signal from all earlier excitations. η is the PL efficiency at a specific emission wavelength, and N is the normalization condition,

$$N=\frac{1}{\int_0^{\infty}\exp\frac{-t'}{\tau}dt'}=\frac{1}{\tau}. \tag{3}$$

Therefore,

$$\zeta_r(t)=\frac{\eta}{\tau}\int_0^{\infty}\frac{\zeta_0}{2}[2-m+m\ \sin\ \hat{\omega}(t-t')]\exp\frac{-t'}{\tau}dt' \tag{4}$$

$$=\frac{\zeta_0\eta}{2}\left(2-m+m\frac{\sin\hat{\omega}t-\tau\hat{\omega}\ \cos\ \tau\hat{\omega}}{1+\tau^2\hat{\omega}^2}\right). \tag{5}$$

Introducing $\theta=\arctan\tau\hat{\omega}$:

$$\zeta_r(t)=\frac{\zeta_0\eta}{2}\left(2-m+m\frac{\sin(\hat{\omega}t+\theta)}{(1+\tau^2\hat{\omega}^2)^{1/2}}\right). \tag{6}$$

Hence the maximum amplitude of the PL intensity signal at the modulation frequency $\hat{\omega}$ is:

$$\zeta_r^{\max}(\hat{\omega})=\frac{\zeta_0\eta m}{2}(1+\tau^2\hat{\omega}^2)^{-1/2} \tag{7}$$

which is the signal detected by a lock-in amplifier. By measuring $\zeta_r^{\max}(\hat{\omega})$ at many different frequencies the lifetime, τ, was calculated by taking a least squares best fit of $(\zeta_r^{\max})^{-2}$ against $\hat{\omega}^2$ (see inset of Fig. 4).

It was desirable to keep the *nipi* band structure in quasiequilibrium during the lifetime measurement. Therefore the modulation depth was kept small ($m=6\%$). cw PL spectra were measured using the modulated laser, and they were found to be indistinguishable from those of the unmodulated laser (Fig. 2), which indicates that the band structure was in quasi-equilibrium.

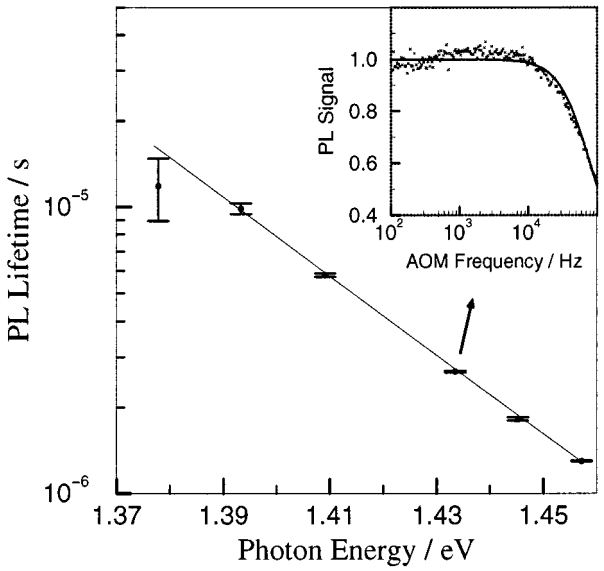

FIG. 4. PL lifetime of a δ-doped sawtooth superlattice measured as a function of PL emission energy. Inset: data used to calculate the lifetime for the 1.43 eV ($\lambda=865$ nm) point of the main figure. The solid curve is Eq. (7) with $\tau=2.67\pm0.02$ μs. $\zeta_0\eta m/2$ in this graph has been normalized to 1.

In contrast with TRPL, which measures the *temporal relaxation* of the sample's band edges, this new technique allows the tunability of the carrier recombination *lifetime* to be shown. That is, the band structure is held in quasiequilibrium during the lifetime measurement. TRPL measures the peak PL, and hence approximate position of band edges, whereas the lifetime technique measures an (exponential) PL lifetime at a specific emission photon energy.

The radiative recombination lifetime was measured for specific states of relaxation of the structure. In each case the intensity, ζ_0, was varied using neutral density filters and then the lifetime was measured at the wavelength corresponding to the continuous PL maximum. These lifetime data are expressed in terms of emission energy of PL in Fig. 4. Thus the abscissa here corresponds directly to the position of the effective band-gap energy of the *nipi*. By comparing Figs. 2 and 4 it can be seen that the PL lifetime of the *nipi* structure varies with excitation intensity. Therefore a tunable PL lifetime has been demonstrated in a sawtooth superlattice between 1.37 eV and 1.45 eV.

It should be noted that data to determine radiative recombination lifetimes were also taken at effective band-gap energies lower than 1.37 eV. There was clearly a decrease in the average lifetime with decreasing energy, but these decays were no longer consistent with a single exponential lifetime [Equation (7)], and hence are inappropriate for Fig. 4.

These recombination lifetime results are still much smaller than theoretical lifetimes determined by methods such as those used by Jonsson *et al.*[13] This discrepancy indicates that extrinsic (nonradiative) recombination most likely plays a significant role in the relaxation of *nipi* structures.

A comparison of Fig. 4 with Fig. 3 is necessary. The decay lifetime is not necessarily dependent on the delay time after excitation. Instead these data give an indication of the rate of recombination of carriers when the effective band gap is at a particular energy. The TRPL on the other hand showed the relaxation of the effective band gap. The fact that the PL lifetime is comparable to the time scale of TRPL data implies that the relaxation process is closely related to the radiative recombination of carriers. That is, the PL lifetime increases as the effective band gap reduces (the structure relaxes); this corresponds to the slowing of the band relaxation at lower band-gap energies which was expressed in the TRPL data.

VII. CONCLUSION

A systematic photoluminescence study of a δ-doped *nipi* has revealed interesting band edge relaxation effects. In addition to the well studied shifting of effective band gap with excitation energy, the temporal evolution of the band edges has been examined. Furthermore, a new technique has been developed which enabled the radiative recombination lifetime to be determined at fixed effective band gaps. These features may find direct application as modulators and tunable light sources, but also act as a starting point into the study of the nonlinearities associated with more complicated structures such as hetero-*nipi*s.

ACKNOWLEDGMENT

The authors wish to thank John Tann for technical assistance and helpful discussions.

[1] L. Esaki and R. Tsu, IBM J. Res. Dev. **14**, 61 (1970).
[2] G. H. Döhler, Phys. Status Solidi B **52**, 79 (1972).
[3] E. F. Schubert, J. E. Cunningham, and W. T. Tsang, Phys. Rev. B **36**, 1348 (1987).
[4] G. Li, C. Jagadish, M. B. Johnston, and M. Gal, Appl. Phys. Lett. **69**, 4218 (1996).
[5] G. H. Döhler, IEEE J. Quantum Electron. **22**, 1682 (1986).
[6] E. F. Schubert, Surf. Sci. **228**, 240 (1990).
[7] N. Moritz, H. M. Hauenstein, and A. Seilmeier, Phys. Rev. B **52**, 17 300 (1995).
[8] E. F. Schubert, Opt. Quantum Electron. **22**, S141 (1990).
[9] H. Vaghjiani, E. A. Johnson, M. J. Kane, R. Grey, and C. C. Phillips, J. Appl. Phys. **76**, 4407 (1994).
[10] H. Ando, H. Iwamura, H. Oohashi, and H. Kanbe, IEEE J. Quantum Electron. **25**, 2135 (1989).
[11] A. Larsson and J. Maserjian, Appl. Phys. Lett. **59**, 1946 (1991).
[12] W. Rehm, P. Ruden, G. H. Döhler, and K. Ploog, Phys. Rev. B **28**, 5937 (1983).
[13] B. Jonsson, A. Larsson, O. Sjölund, S. Wang, T. G. Anderson, and J. Marerjian, IEEE J. Quantum Electron. **30**, 63 (1994).
[14] E. Schubert, J. Kuo, and R. Kopf, J. Electron. Mater. **19**, 521 (1990).
[15] G. H. Döhler, G. Fasol, and J. N. Miller, Solid State Commun. **57**, 563 (1986).